

Non-Hermitian synthetic lattices with light-matter couplingAmir Rahmani ¹, Mateusz Kędziora ², Andrzej Opala ^{1,2} and Michał Matuszewski¹¹*Institute of Physics Polish Academy of Sciences, Aleja Lotników 32/46, 02-668 Warsaw, Poland*²*Institute of Experimental Physics, Faculty of Physics, University of Warsaw, ulica Pasteura 5, PL-02-093 Warsaw, Poland*

(Received 9 January 2023; revised 16 March 2023; accepted 12 April 2023; published 26 April 2023)

We propose that light-matter coupling can be used to realize synthetic lattices. In particular, we consider a one-dimensional chain of exciton-photon sites to create a comb lattice that exhibits a transition from a flat band to a finite mass dispersion by tuning site-dependent light-matter coupling. Moreover, in a non-Hermitian system with gain and loss, the flat-band phase is much more robust, and the transition is accompanied by the appearance of exceptional points in the complex energy spectrum. We demonstrate that by engineering the light-matter coupling in the synthetic lattice, one can explore various phases in the lasing regime. Our proposal paves the way for studying non-Hermitian systems in higher dimensions.

DOI: [10.1103/PhysRevB.107.165309](https://doi.org/10.1103/PhysRevB.107.165309)**I. INTRODUCTION**

Lattice models are ubiquitous in physics with applications ranging from approximations of real physical systems to efficient tools in theoretical research, such as lattice gauge theory. In the context of quantum simulation, synthetic lattices are highly beneficial as a method for using the internal degree of freedoms [1] or external states [2] to investigate nontrivial topology and higher dimensions [1,3]. The formation of different lattice configurations may be implemented by using spin [4], Rydberg states [5], orbital angular momentum states [6,7], and photonic frequency comb [8].

Light-matter coupling may provide an advantage in investigations of non-Hermitian physics [9] due to flows of energy or particles to and from a system. A key feature of non-Hermitian systems is the presence of complex eigenvalues, which can lead to a variety of interesting phenomena, such as nonreciprocal transport [10], topological phases [11], and exceptional points [12]. A possible non-Hermitian system is a lattice with gain and loss at its sites [13,14]. Here we explore how light-matter coupling can provide an additional degree of freedom for creating a synthetic lattice. We study a simple model of a one-dimensional lattice in which the light-matter coupling can be manipulated. As such, we provide an example of a comb lattice. In one dimension, the lattice can be obtained from a two-leg ladder lattice [15] by removing one leg whereas keeping all other connections and couplings unchanged. Such lattices have been explored in the context of random walks [16] and modeling chemical compounds [17].

Light can couple to matter both weakly or strongly in the latter case leading to hybrid light-matter quasiparticles called polaritons [18,19]. Lattices of photonic nodes can be created by structuring the sample itself by deposition of a patterned layer on top of a cavity, sample etching [20], or etch-and-overgrowth [21] procedures as well as using a spatial light modulator to excite selected nodes [22]. The ease of creating arbitrary geometries and potential landscapes in polariton systems opened the way for studying a variety of Hamiltonian models, including Lieb lattices [23–32],

kagome [21], and honeycomb [20,33] lattices, as well as one-dimensional [34,35] and two-dimensional [36] topological systems. Owing to the possibility to manipulate gain and loss [37,38] polaritons are an ideal system for studying non-Hermitian effects [39]. A growing interest in such systems is directly related to the possibility of exploring the physics of exceptional points [12,40–42], parity-time symmetry [43], or skin effect [10,44–46].

In this paper, we propose that light-matter coupling in the intermediate regime between strong and weak coupling can be exploited to introduce a synthetic lattice with nontrivial properties. The considered lattice, schematically shown in Fig. 1, is synthetic in the sense that it can be engineered to possess specific features, such as lasing and flat bands. The fact that photon and exciton modes in the same micropillar couple allows to describe the system formally as a one-legged comb model. This allows investigation of the physics of a Lieb (Stub) lattice, including the appearance of a flat band. We show that site-dependent tuning of light-matter coupling strength allows the observation of the transition from a flat band to a dispersive spectrum.

Moreover, by analyzing the properties of the system in the more realistic non-Hermitian regime with gain and loss included, we find that the difference in loss rates between excitons and photons leads to a great enhancement of robustness of the flat-band phase, and the appearance of a new flat band in a strongly non-Hermitian case. These effects are shown to persist in the nonlinear regime of lasing where the signatures of a flat band and associated compact localized states [47] (CLS) can be observed in a state resulting from a long-time evolution starting from a random initial condition.

Our results show that manipulating the light-matter coupling strength in lattices opens the way for the experimental realization of a new kind of synthetic lattices that allow to explore strongly non-Hermitian physics. Our model can be easily extended to higher dimensions or a larger number of light and matter states, such as orthogonal light polarizations or higher exciton states [48,49]. It can be implemented in other physical platforms, such as cavity quantum

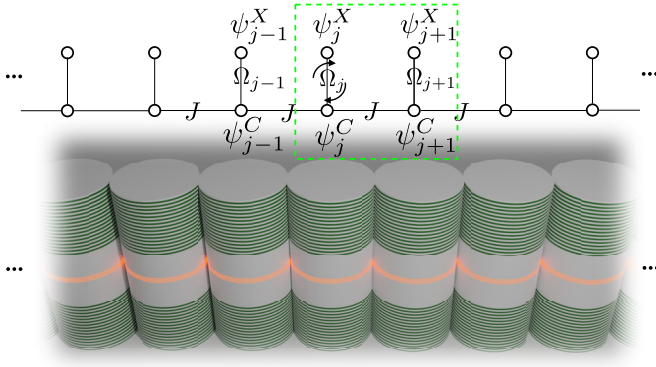


FIG. 1. Scheme of our model. (Top) At lattice site j photonic (ψ_j^C) and excitonic (ψ_j^X) states are coupled. The neighboring photonic sites are coupled to each other with coupling rate J . A possible choice of a unit cell is marked by the green square. (Bottom) In practice the model can be implemented in a lattice of coupled micropillars.

electrodynamics [50] and coupled atom-light systems [51]. We believe that our proposal may lead to engineering highly dimensional extended lattices, providing an ideal platform for simulators of complex non-Hermitian models.

II. MODEL

The lattice described by our model shown in Fig. 1, consists of $2N$ micropillars (N is the cell index with two micropillars per unit cell) forming a one-dimensional chain with lattice constant a . Each site is described with two components where we label exciton components with superscript X and photonic components with superscript C . We assume that there is finite and uniform coupling between the sites via photonic components, whereas exciton components are not coupled with each other due to the much larger exciton effective mass. Photon and exciton modes in the same site are coupled with each other with the strength corresponding to Rabi frequencies which vary from site to site. We consider a staggered distribution of couplings denoted by Ω_1 in odd-numbered sites and Ω_2 in even-numbered sites, where $\Omega_2 \leq \Omega_1$. In particular, such a position-dependent light-matter coupling can be realized in practice using site-dependent external pumping, which induces saturation of Rabi coupling [52]. Photon tunneling between photon modes localized in neighboring micropillars is described with J . As result, the model describing the system can be considered effectively two dimensional with an additional two-site exciton-photon degree of freedom.

Our model equations can be presented in terms of four fields inside a unit cell. Denoting each cell with index $n = 1-3, \dots, N$, we have $2N$ micropillars, for which we introduce fields ψ_j^C, ψ_j^X corresponding to photon and exciton components at site j , where $j = 1, 2, \dots, 2N$. The mean-field evolution equations are

$$i \partial_t \psi_j^C = -i\gamma_C \psi_j^C + J(\psi_{j-1}^C + \psi_{j+1}^C) + \Omega_j \psi_j^X, \quad (1a)$$

$$i \partial_t \psi_j^X = -i\gamma_X \psi_j^X + g\hbar^{-1} |\psi_j^X|^2 \psi_j^X + \Omega_j \psi_j^C, \quad (1b)$$

where $\Omega_j = \Omega_1$ for odd j and $\Omega_j = \Omega_2$ for even j , $\gamma_C (\gamma_X)$ denotes the decay rate from the photon (exciton) modes, and g is the nonlinear coefficient. Here g is a complex number taking into account both exciton-exciton interaction in its real part and gain saturation effect in its imaginary part [42]. In the case of periodic boundary conditions we assume $\psi_{N+1}^C = \psi_1^C$. For simplicity, we consider the case where there is no exciton-photon detuning at any site.

To calculate the spectrum of the system, we consider the eigenvalue equation $\tilde{H}\tilde{\Psi} = E(k)\tilde{\Psi}$ at $g = 0$, where $\tilde{\Psi}$ is a plane wave solution with momentum k . We obtain

$$\tilde{H} = \begin{pmatrix} -i\hbar\gamma_C & \hbar\Omega_1 & \hbar J(1 + e^{-ika}) & 0 \\ \hbar\Omega_1 & -i\hbar\gamma_X & 0 & 0 \\ \hbar J(1 + e^{ika}) & 0 & -i\hbar\gamma_C & \hbar\Omega_2 \\ 0 & 0 & \hbar\Omega_2 & -i\hbar\gamma_X \end{pmatrix}. \quad (2)$$

In the following, we will analyze in detail the properties of the system in both linear and nonlinear regimes.

III. HERMITIAN CASE

For the sake of clarity, we start our study with the linear Hermitian case $\gamma_C = \gamma_X = 0$ and $g = 0$. When $\Omega_2 = 0$, even exciton nodes ψ_{2n}^X are completely isolated from all other nodes. The remaining photonic nodes and odd exciton nodes form the so-called one-dimensional Lieb lattice (also called the Stub lattice) model [24,53,54]. In this case one can find the dispersion equation analytically, $E(k) = 0, \pm\hbar\sqrt{\Omega_1^2 + 2J^2[1 + \cos(ka)]}$. The model exhibits a flat band with $E = 0$ and infinite mass separated by gaps from two dispersive bands, see Fig. 2(a). Flat bands possess a number of intriguing physical phenomena, including compact localized states, sensitivity to perturbations and disorder, strongly correlated phases, and topological states [47]. Note that in addition to the Lieb lattice flat band, the full model (1) has a trivial flat band that corresponds to isolated exciton sites.

When the Ω_2 parameter is nonzero, the two degenerate flat bands at $E = 0$ split into two dispersive bands as shown in Figs. 2(b) and 2(c). Hence, in the Hermitian case, flat bands are present only in the limit of $\Omega_2 = 0$. On the other hand, in the symmetric case, $\Omega_1 = \Omega_2$, the two bands with positive energy and the two bands with negative energy coalesce with each other, marking a transition to the uniform one-legged ladder model. In the intermediate regime $0 < \Omega_2 < 1$, the two middle bands that emerged from the flat bands preserve some properties of the flat-band eigenstates. In particular, the structure of the eigenstates in the middle bands resembles the CLS of the Lieb lattice as in Fig. 2(d). In contrast, the eigenstates of the dispersive top and bottom bands resemble standard bulk states, see Fig. 2(e).

IV. LINEAR NON-HERMITIAN CASE

We analyze the effect of nonzero decay γ_C, γ_X on the spectra and eigenstates of the system, keeping the interactions $g = 0$. The results are presented in Fig. 3. It should be noted that adding a uniform decay rate $\gamma_C = \gamma_X > 0$ would lead only to

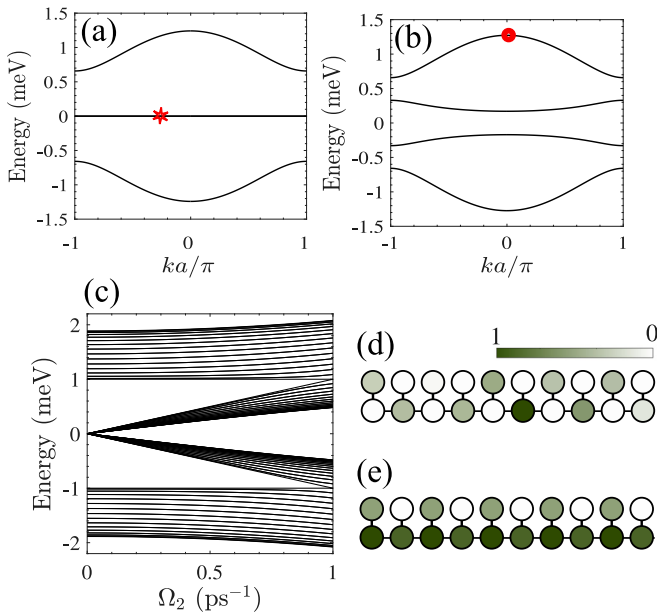


FIG. 2. Examples of spectra and eigenstates in the linear Hermitian case. (a) and (b) Energy spectra in momentum space for an infinite system. In (a) we assume $\Omega_2 = 0$ (Stub lattice). In this case there are two degenerate flat bands with $E = 0$, one corresponding to the Lieb lattice flat band, and another corresponding to isolated exciton sites ψ_{2n}^X . In (b) we have $\Omega_2 = 0.4 \text{ ps}^{-1}$, and the flat bands split into two dispersive bands. Panel (c) shows an eigenenergy spectrum in function of Ω_2 in a finite system with $N = 30$. (d) and (e) Examples of density distributions for eigenstates corresponding to the flat band in (a) and dispersive band in (b), respectively. Corresponding points are marked with a red star and a circle in (a) and (b). Color scale is in arbitrary units. Other parameters are $\Omega_1 = 1 \text{ ps}^{-1}$, $J = 0.8 \text{ ps}^{-1}$.

an addition of a constant imaginary part to the eigenvalues of the system with no effect on the real part of the spectrum or the eigenfunctions. However, in real systems the decay rate of photons γ_C is typically much higher than the decay rate for excitons γ_X . We find that this leads to a dramatic change in the spectra. An example is shown in Figs. 3(a) and 3(b) where real and imaginary parts of eigenenergies are shown for the same parameters as in the Hermitian case of Fig. 2(b), but with $\gamma_C = 2.2 \text{ ps}^{-1}$ and $\gamma_X = 0.1 \text{ ps}^{-1}$. In contrast to the Hermitian case, we find that despite nonzero Ω_2 , the system spectrum contains two flat bands in the entire Brillouin zone, whereas the dispersive bands develop small regions of flat dispersion at the two ends of the Brillouin zone. The transition from dispersive dependence at low quasimomentum to purely imaginary dependence at high quasimomenta is marked by the occurrence of exceptional points. We note that previously a purely imaginary dispersion was predicted to occur in the Bogoliubov excitation spectrum of a polariton condensate coupled to a reservoir [55]. However, it occurs at low momenta whereas the miniflat bands that appear in our model are present at high quasimomenta, and the model does not assume condensation or include interactions with an uncondensed reservoir.

The real part of energy eigenvalues is presented as a function of Ω_2 in Figs. 3(c) and 3(d) for two values of the photon

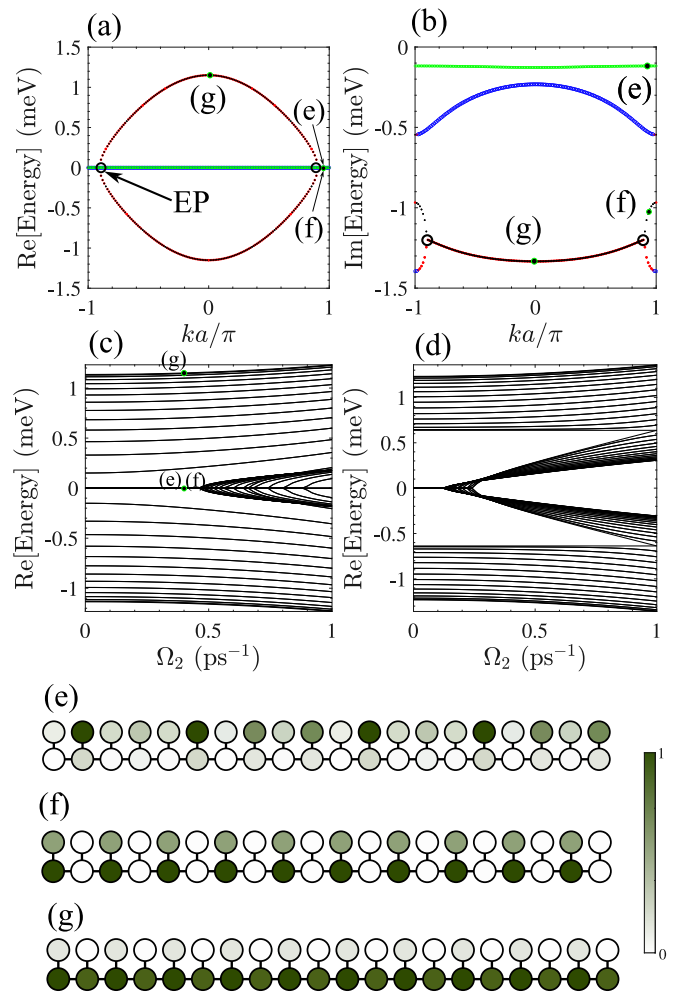


FIG. 3. Linear non-Hermitian case. In (a) and (b) we show the real and imaginary parts of eigenvalues in a function of quasimomentum for the same parameters as in Fig. 2(b), but with nonzero decay terms $\gamma_C = 2.2 \text{ ps}^{-1}$ and $\gamma_X = 0.1 \text{ ps}^{-1}$. In contrast to the Hermitian case, flat bands are present in the system for a nonzero coupling $\Omega_2 = 0.4 \text{ ps}^{-1}$. Exceptional points are marked with a black open circle. In (c) and (d) we show real parts of eigenvalues in function of Ω_2 for the fixed $\Omega_1 = 1 \text{ ps}^{-1}$. Qualitatively different spectra are shown in (d) for a smaller decay rate $\gamma_C = 0.54 \text{ ps}^{-1}$. The eigenstates corresponding to the points marked in panels (a) and (b) are shown in panels (e)–(g).

decay rate γ_C . Upon changing the decay rate, exceptional points may emerge in the spectrum. Although in the case of a high decay rate there are no energy gaps in the real part of the energy, in the low decay rate case the gaps are open at low values of Ω_2 and the system spectrum is more similar to the Hermitian case of Fig. 2(c). Nevertheless, even in this case flat bands survive to a nonzero value of Ω_2 , in contrast to the Hermitian limit. This shows that including dissipation to the model, which occurs naturally in photonic systems, makes flat bands much more robust. Moreover, increasing γ_C may induce exceptional points. At low decay rates, we have three distinct bands (including a flat band). This is shown in panel (d) for low values of Ω_2 . But by increasing the decay rate, the band gaps start decreasing, whereas exceptional points

emerge at the gap closing. An example of a gapless spectrum is shown in panel (c). In general, increasing decay rate leads to coalescence of eigenvalues which gives rise to exceptional points and the disappearance of the gap. At larger values of the decay rate, exceptional points are present for any value of Ω_2 , and so the real part has no gap in panel (c). However, for a lower value of the decay rate the exceptional points may appear only at certain range of Ω_2 . For this reason, the spectrum in panel (d) displays band gaps.

Finally, in Figs. 3(e)–3(g) we show three examples of density distributions of eigenstates corresponding to different bands. The eigenstate of the flat band shown in Fig. 3(e) preserves the characteristic structure of the CLS of the Hermitian model, with all odd photonic sites being empty. In contrast, the state from the flat miniband at high quasimomentum in Fig. 3(f) is characterized by a complementary pattern with all even photonic sites being empty. An eigenstate from the dispersive band in the center of the Brillouin zone depicted in Fig. 3(g) shows no particular structure of photonic states, which are distributed more or less uniformly with only a small admixture of excitonic states.

V. LASING

In the previous section we considered a lattice in the linear non-Hermitian regime. A natural extension is a system in the presence of nonlinearity $g \neq 0$. Lasing corresponds to a steady state in the case of positive gain. To achieve the steady-state regime, we add a new feature to our dissipative model, that is, we consider a balance between gain and nonlinear decay. In this case particles escaping the lattice can be replenished by a pumping term.

This can be analyzed simply by assuming $\gamma_X < 0$ (as the pump source, e.g., a nonresonant optical pump creating excitons) whereas $\gamma_C > 0$ (photon decay). In this regime, we need to assume a nonzero-complex nonlinear term ($g \neq 0$) in Eqs. (1) to reach a stable steady state. We keep the associated parameters in the so-called weak nonlinear regime when $|g||\psi_{1,n}|^2$ and $|g||\psi_{2,n}|^2$ are, at least, one order of magnitude lower than $\hbar\gamma_C$. As an aside, one possible source of disorder that may become important in our modeling is due to randomness in pumping, which is not considered here, but the results remain unchanged with a minor percent of disorder strength [56]. We provide examples of the dynamics in the steady-state regime in Fig. 4.

Additionally, we calculate the spectrum of small Bogoliubov excitations around the steady state. As we are dealing with a homogeneous case, in the steady-state case we may consider a stationary solution in the form $\psi_j^{SC,SX} e^{-iEt/\hbar}$. The phase factor holds information about the eigenvalues of the model in real space. Indeed, by substituting the above ansatz in Eq. (1), one can find a set of time-independent equations,

$$0 = (-i\hbar\gamma_C - E)\psi_j^{SC} + \hbar J(\psi_{j-1}^{SC} + \psi_{j+1}^{SC}) + \hbar\Omega_j\psi_j^{SX}, \quad (3a)$$

$$0 = (-i\hbar\gamma_X - E)\psi_j^{SX} + \hbar\Omega_j\psi_j^{SC} + g|\psi_j^{SX}|^2\psi_j^{SX}, \quad (3b)$$

which can be solved to find the eigenvalues E . To this end, we solve model equations [Eq. (1)] numerically by employing Runge-Kutta method, and use the corresponding excitonic

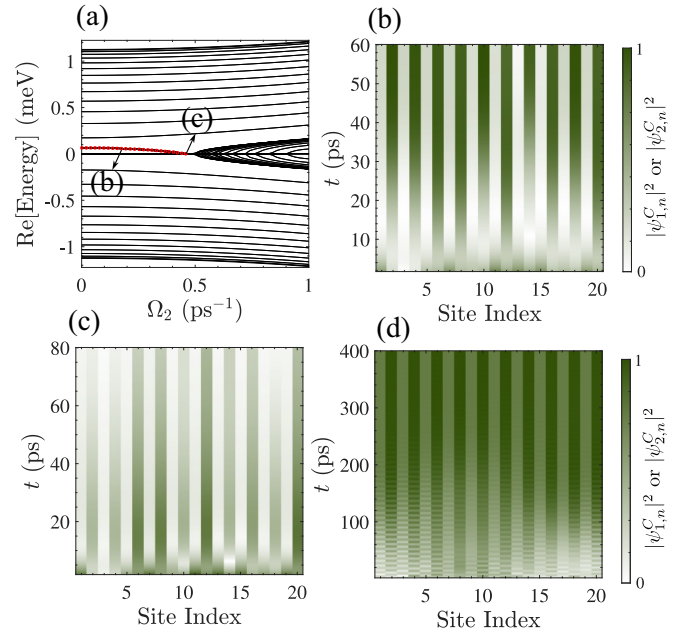


FIG. 4. (a) Real part of energy of excitations in a nonlinear steady state in a function of Ω_2 for $N = 30$. The system is in the weakly nonlinear regime. Parameters are $\gamma_C = 2.2 \text{ ps}^{-1}$ and $\gamma_X = -0.1 \text{ ps}^{-1}$, other parameters as in Fig. 3. Red dots show the energy of the linear excitation mode with the zero imaginary part. All other excitations have energies with negative imaginary parts. In panels (b)–(d) we show the evolution of densities in photonic sites. In panel (b) we used $\Omega_2 = 0.18 \text{ ps}^{-1}$, which corresponds to a nonzero real eigenenergy, see panel (a). In panel (c) we used $\Omega_2 = 0.46 \text{ ps}^{-1}$ for which the real part of the energy is very near the zero-energy flat band. The resulting density shows signatures of random localization. Panel (d) shows an example of dynamics in a weakly dissipative case where we used $\gamma_C = 0.54 \text{ ps}^{-1}$, $\gamma_X = -0.12 \text{ ps}^{-1}$, and $\Omega_2 = 0.85 \text{ ps}^{-1}$. Here the system reaches the steady state after initial Rabi oscillations. We assume the nonlinear parameter $\hbar g = 0.005 - 0.005i \text{ meV}^2 \text{ ps}$, which consists of both density-preserving interactions and density-dependent decay.

occupations in the steady-state solution $|\psi^{SX}|^2$ in the above equations.

In the steady state, we are interested in excitations for which the imaginary part of the energy eigenvalue $\text{Im}[E]$ is zero since for $\text{Im}[E] > 0$ the steady state is unstable, and for $\text{Im}[E] < 0$ the excitations decay in time. Excitation modes with $\text{Im}[E] = 0$ can be considered as discrete analogs of Goldstone modes. We assume that the parameter that can be manipulated externally is Ω_j . As such, it would be useful to consider the variations in energies with Ω_2 in a steady state.

Real parts of excitation eigenvalues are shown in Fig. 4(a). Here we assume that the interactions in a chain of micropillars are effectively repulsive via the effect of exciton-exciton interactions. Considering the case when particle-conserving interactions and gain saturation are of the same order of magnitude, we choose $\hbar g = 0.005 - 0.005i \text{ meV}^2 \text{ ps}$ as our effective nonlinear parameter taking into account both conservative and dissipative nonlinear processes. We note that in comparison to the linear case in Fig. 3(c), at small Ω_2 a new split band is present in Fig. 4(a). This splitting from the

zero-energy band is a nonlinear effect, that is, the nonlinear term induces a positive on-site potential for the excitons, proportional to $\text{Re}[g]|\psi_j^X|^2$. We note that for small Ω_2 exciton sites which are indexed by $j = 2n$ are almost isolated from the rest of the lattice. Since excitons at these sites do not experience photonic decay γ_C , their decay is controlled by the imaginary part of the nonlinear term $g|\psi_j^X|^2$. This term is much smaller than the decay of photonic states γ_C in the case of the weakly nonlinear regime that we consider here. Hence, the $j = 2n$ excitonic sites experience the highest gain, which results in a steady state where density is mostly localized at these sites at small Ω_2 . We show an example of steady-state formation starting from a random initial condition in Fig. 4(b).

As Ω_2 increases, these disconnected excitonic states (ψ_{2n}^X) couple strongly with the other states. The populations in the other sites in the steady state increase whereas the population in ψ_{2n}^X decreases. At some critical Ω_2 the split band gap is closed, and the real part of the energy eigenvalue becomes zero as visible in Fig. 4(a). At this point, the eigenstate of the system with the highest imaginary part of the energy belongs to the $E = 0$ flat band. This has a profound effect on the dynamics of the system. As shown in Fig. 4(c), states that are spontaneously formed from a random initial condition result in a different random density distribution after some certain time. This random density distribution is long lived and locally resembles the density of a flat-band state. This can be seen as a reminiscence of flat-band CLS of the linear Lieb model, see Fig. 2(d). Further increasing Ω_2 with other parameters fixed leads to a situation where no steady state exists since all the eigenstates have negative imaginary parts. In this case any initial distribution decays to zero. A qualitatively different situation occurs where the photon decay is decreased as shown in Fig. 4(d). In this case the system converges to a steady state with a periodic regular density distribution with all sites occupied. The initial dynamics shows a clear signature of collective Rabi oscillations in the lattice, which decays after a sufficiently long time.

VI. CONCLUSION

To summarize, we propose that a lattice system with coupled light, and matter modes can be used to realize a synthetic comb lattice by employing the internal degree of freedom due to light-matter coupling. This idea can be readily realized in exciton-polariton systems where several methods of tuning light-matter coupling strength have been shown. We

demonstrated that local engineering of light-matter coupling provides a way to explore a dissipative phase transition between the regimes of dispersive and flat-band phases. The transition is accompanied by the appearance of exceptional points in the spectrum. Importantly, in the dissipative case the flat-band regime is not restricted to a limiting case in the parameter space but exists in a range of values of light-matter coupling, which makes the phenomenon much more robust than in the Hermitian case. We also showed that the existence of a flat band has a profound effect on the states of the system after long evolution in the regime of lasing, enabling a straightforward experimental observation. The proposed method can be generalized to higher-dimensional lattices, and the number of sites in the synthetic lattice can be increased by considering additional light and matter states. This opens the way to explore non-Hermitian systems in higher dimensions.

ACKNOWLEDGMENT

A.R., M.K., and M.M. acknowledge support from National Science Center, Poland (PL), Grant No. 2016/22/E/ST3/00045, A.O. acknowledges Grant No. 2019/35/N/ST3/01379.

APPENDIX

The dynamics of exciton-polaritons are known to be described by mean-field Gross-Pitaevskii equations,

$$i\hbar \partial_t \psi^C = -i\hbar\gamma_C \psi^C + \hbar\Omega \psi^X, \quad (\text{A1a})$$

$$i\hbar \partial_t \psi^X = (-\delta - i\hbar\Gamma_X) \psi^X + \hbar\Omega \psi^C + \alpha_1 |\psi^X|^2 \psi^X + g_R n_R \psi^X + i\hbar R n_R \psi^X, \quad (\text{A1b})$$

$$\partial_t n_R = P - (\gamma_R + R |\psi^X|^2) n_R, \quad (\text{A1c})$$

where n_R is the density of the exciton reservoir, $P(\gamma_R)$ is the rate of pumping to (decay from) a reservoir. There are three parameters that take into account interactions: α_1 , g_R , and R . The energy detuning between the exciton and the photon field is given by δ . By using the adiabatic approximation [57] one can assume that $n_R \approx \frac{P}{\gamma_R} (1 - \frac{R |\psi^X|^2}{\gamma_R})$, the effective equation for the exciton field becomes

$$i\hbar \partial_t \psi^X = -i\hbar\gamma_X \psi^X + \hbar\Omega \psi^C + g |\psi^X|^2 \psi^X, \quad (\text{A2})$$

where we introduce $-i\hbar\gamma_X = -\delta - i\hbar\Gamma_X + P/\gamma_R(g_R + i\hbar R)$, $g = \alpha_1 - \frac{g_R P}{\gamma_R} - i \frac{\hbar R^2 P}{\gamma_R^2}$. Equation (A2) has been used to simulate the exciton field in the main text.

- [1] O. Boada, A. Celi, J. I. Latorre, and M. Lewenstein, Quantum Simulation of an Extra Dimension, *Phys. Rev. Lett.* **108**, 133001 (2012).
- [2] H. M. Price, T. Ozawa, and N. Goldman, Synthetic dimensions for cold atoms from shaking a harmonic trap, *Phys. Rev. A* **95**, 023607 (2017).
- [3] T. Ozawa and H. M. Price, Topological quantum matter in synthetic dimensions, *Nat. Rev. Phys.* **1**, 349 (2019).
- [4] A. Celi, P. Massignan, J. Ruseckas, N. Goldman, I. B. Spielman, G. Juzeliūnas, and M. Lewenstein, Synthetic Gauge

Fields in Synthetic Dimensions, *Phys. Rev. Lett.* **112**, 043001 (2014).

- [5] S. K. Kanungo, J. D. Whalen, Y. Lu, M. Yuan, S. Dasgupta, F. B. Dunning, K. R. A. Hazzard, and T. C. Killian, Realizing topological edge states with rydberg-atom synthetic dimensions, *Nat. Commun.* **13**, 972 (2022).
- [6] J. Floß, A. Kamalov, I. S. Averbukh, and P. H. Bucksbaum, Observation of Bloch Oscillations in Molecular Rotation, *Phys. Rev. Lett.* **115**, 203002 (2015).
- [7] B. Sundar, B. Gadway, and K. R. A. Hazzard, Synthetic dimensions in ultracold polar molecules, *Sci. Rep.* **8**, 3422 (2018).

- [8] Q. Lin, M. Xiao, L. Yuan, and S. Fan, Photonic Weyl point in a two-dimensional resonator lattice with a synthetic frequency dimension, *Nat. Commun.* **7**, 13731 (2016).
- [9] Y. Ashida, Z. Gong, and M. Ueda, Non-hermitian physics, *Adv. Phys.* **69**, 249 (2020).
- [10] S. Mandal, R. Banerjee, and T. C. H. Liew, From the topological spin-hall effect to the non-hermitian skin effect in an elliptical micropillar chain, *ACS Photonics* **9**, 527 (2022).
- [11] Z. Gong, Y. Ashida, K. Kawabata, K. Takasan, S. Higashikawa, and M. Ueda, Topological Phases of Non-Hermitian Systems, *Phys. Rev. X* **8**, 031079 (2018).
- [12] M.-A. Miri and A. Alù, Exceptional points in optics and photonics, *Science* **363**, eaar7709 (2019).
- [13] A. Szameit, M. C. Rechtsman, O. Bahat-Treidel, and M. Segev, \mathcal{PT} -symmetry in honeycomb photonic lattices, *Phys. Rev. A* **84**, 021806(R) (2011).
- [14] K. Takata and M. Notomi, Photonic Topological Insulating Phase Induced Solely by Gain and Loss, *Phys. Rev. Lett.* **121**, 213902 (2018).
- [15] R. Ye, G. Li, L. Wang, X. Wu, L. Yuan, and X. Chen, Controlling localized states in a two-leg ladder lattice with diagonal edges via gain/loss, *Opt. Mater. Express* **12**, 4755 (2022).
- [16] P. Illien and O. Bénichou, Propagators of random walks on comb lattices of arbitrary dimension, *J. Phys. A: Math. Theor.* **49**, 265001 (2016).
- [17] K. Shida, A. Kasuya, K. Ohno, Y. Kawazoe, and Y. Nakamura, Monte carlo calculation of second and third virial coefficients of small-scale comb polymers on lattice, *J. Chem. Phys.* **126**, 154901 (2007).
- [18] J. J. Hopfield, Theory of the contribution of excitons to the complex dielectric constant of crystals, *Phys. Rev.* **112**, 1555 (1958).
- [19] C. Weisbuch, M. Nishioka, A. Ishikawa, and Y. Arakawa, Observation of the Coupled Exciton-Photon Mode Splitting in a Semiconductor Quantum Microcavity, *Phys. Rev. Lett.* **69**, 3314 (1992).
- [20] T. Jacqmin, I. Carusotto, I. Sagnes, M. Abbarchi, D. D. Solnyshkov, G. Malpuech, E. Galopin, A. Lemaître, J. Bloch, and A. Amo, Direct Observation of Dirac Cones and a Flatband in a Honeycomb Lattice for Polaritons, *Phys. Rev. Lett.* **112**, 116402 (2014).
- [21] T. H. Harder, O. A. Egorov, C. Krause, J. Beierlein, P. Gagel, M. Emmerling, C. Schneider, U. Peschel, S. Höfling, and S. Klembt, Kagome flatbands for coherent exciton-polariton lasing, *ACS Photonics* **8**, 3193 (2021).
- [22] L. Pickup, H. Sigurdsson, J. Ruostekoski, and P. G. Lagoudakis, Synthetic band-structure engineering in polariton crystals with non-hermitian topological phases, *Nat. Commun.* **11**, 4431 (2020).
- [23] C. E. Whittaker, E. Cancellieri, P. M. Walker, D. R. Gulevich, H. Schomerus, D. Vaitiekus, B. Royall, D. M. Whittaker, E. Clarke, I. V. Iorsh, I. A. Shelykh, M. S. Skolnick, and D. N. Krizhanovskii, Exciton Polaritons in a Two-Dimensional Lieb Lattice with Spin-Orbit Coupling, *Phys. Rev. Lett.* **120**, 097401 (2018).
- [24] F. Baboux, L. Ge, T. Jacqmin, M. Biondi, E. Galopin, A. Lemaître, L. Le Gratiet, I. Sagnes, S. Schmidt, H. E. Türeci, A. Amo, and J. Bloch, Bosonic Condensation and Disorder-Induced Localization in a Flat Band, *Phys. Rev. Lett.* **116**, 066402 (2016).
- [25] C. Li, F. Ye, X. Chen, Y. V. Kartashov, A. Ferrando, L. Torner, and D. V. Skryabin, Lieb polariton topological insulators, *Phys. Rev. B* **97**, 081103(R) (2018).
- [26] M. Sun, I. Savenko, S. Flach, and Y. Rubo, Excitation of localized condensates in the flat band of the exciton-polariton lieb lattice, *Phys. Rev. B* **98**, 161204(R) (2018).
- [27] C. E. Whittaker, D. R. Gulevich, D. Biegańska, B. Royall, E. Clarke, M. S. Skolnick, I. A. Shelykh, and D. N. Krizhanovskii, Optical and magnetic control of orbital flat bands in a polariton lieb lattice, *Phys. Rev. A* **104**, 063505 (2021).
- [28] F. Baboux, D. De Bernardis, V. Goblot, V. Gladilin, C. Gomez, E. Galopin, L. Le Gratiet, A. Lemaître, I. Sagnes, I. Carusotto *et al.*, Unstable and stable regimes of polariton condensation, *Optica* **5**, 1163 (2018).
- [29] Q. Fontaine, D. Squizzato, F. Baboux, I. Amelio, A. Lemaître, M. Morassi, I. Sagnes, L. Le Gratiet, A. Harouri, M. Wouters, I. Carusotto, A. Amo, M. Richard, A. Minguzzi, L. Canet, S. Ravets, and J. Bloch, Kardar–parisi–zhang universality in a one-dimensional polariton condensate, *Nature (London)* **608**, 687 (2022).
- [30] F. Scafirimuto, D. Urbonas, M. A. Becker, U. Scherf, R. F. Mahrt, and T. Stöferle, Tunable exciton–polariton condensation in a two-dimensional lieb lattice at room temperature, *Commun. Phys.* **4**, 39 (2021).
- [31] T. H. Harder, O. A. Egorov, J. Beierlein, P. Gagel, J. Michl, M. Emmerling, C. Schneider, U. Peschel, S. Höfling, and S. Klembt, Exciton-polaritons in flatland: Controlling flatband properties in a lieb lattice, *Phys. Rev. B* **102**, 121302(R) (2020).
- [32] P. Deuar, A. Ferrier, M. Matuszewski, G. Orso, and M. H. Szymańska, Fully quantum scalable description of driven-dissipative lattice models, *PRX Quantum* **2**, 010319 (2021).
- [33] M. Milićević, T. Ozawa, P. Andreakou, I. Carusotto, T. Jacqmin, E. Galopin, A. Lemaître, L. L. Gratiet, I. Sagnes, J. Bloch, and A. Amo, Edge states in polariton honeycomb lattices, *2D Mater.* **2**, 034012 (2015).
- [34] P. St-Jean, V. Goblot, E. Galopin, A. Lemaître, T. Ozawa, L. Le Gratiet, I. Sagnes, J. Bloch, and A. Amo, Lasing in topological edge states of a one-dimensional lattice, *Nat. Photonics* **11**, 651 (2017).
- [35] M. Pieczarka, E. Estrecho, S. Ghosh, M. Wurdack, M. Steger, D. W. Snoke, K. West, L. N. Pfeiffer, T. C. H. Liew, A. G. Truscott, and E. A. Ostrovskaya, Topological phase transition in an all-optical exciton-polariton lattice, *Optica* **8**, 1084 (2021).
- [36] S. Klembt, T. H. Harder, O. A. Egorov, K. Winkler, R. Ge, M. A. Bandres, M. Emmerling, L. Worschech, T. C. H. Liew, M. Segev, C. Schneider, and S. Höfling, Exciton-polariton topological insulator, *Nature (London)* **562**, 552 (2018).
- [37] M. D. Fraser, H. H. Tan, Y. d. V. I. Redondo, H. Kavuri, E. A. Ostrovskaya, C. Schneider, S. Höfling, Y. Yamamoto, and S. Tarucha, Independent tuning of exciton and photon energies in an exciton–polariton condensate by proton implantation-induced interdiffusion, *Adv. Opt. Mater.* **11**, 2201569 (2023).
- [38] J. Hu, Z. Wang, N. Lydick, F. Jabeen, C. Schneider, S. Höfling, and H. Deng, Grating-based microcavity with independent control of resonance energy and linewidth for non-hermitian polariton system, *Appl. Phys. Lett.* **121**, 081106 (2022).
- [39] S. Mandal, R. Banerjee, E. A. Ostrovskaya, and T. C. H. Liew, Nonreciprocal Transport of Exciton Polaritons in a Non-Hermitian Chain, *Phys. Rev. Lett.* **125**, 123902 (2020).

- [40] S. Richter, H.-G. Zirnstein, J. Zúñiga Pérez, E. Krüger, C. Deparis, L. Trefflich, C. Sturm, B. Rosenow, M. Grundmann, and R. Schmidt-Grund, Voigt Exceptional Points in an Anisotropic ZnO-Based Planar Microcavity: Square-Root Topology, Polarization Vortices, and Circularity, *Phys. Rev. Lett.* **123**, 227401 (2019).
- [41] R. Su, E. Estrecho, D. Biegańska, Y. Huang, M. Wurdack, M. Pieczarka, A. G. Truscott, T. C. H. Liew, E. A. Ostrovskaya, and Q. Xiong, Direct measurement of a non-hermitian topological invariant in a hybrid light-matter system, *Sci. Adv.* **7**, eabj8905 (2021).
- [42] P. Comaron, V. Shahnazaryan, W. Brzezicki, T. Hyart, and M. Matuszewski, Non-hermitian topological end-mode lasing in polariton systems, *Phys. Rev. Res.* **2**, 022051(R) (2020).
- [43] Ş. K. Özdemir, S. Rotter, F. Nori, and L. Yang, Parity-time symmetry and exceptional points in photonics, *Nature Mater.* **18**, 783 (2019).
- [44] X. Zhu, H. Wang, S. K. Gupta, H. Zhang, B. Xie, M. Lu, and Y. Chen, Photonic non-hermitian skin effect and non-bloch bulk-boundary correspondence, *Phys. Rev. Res.* **2**, 013280 (2020).
- [45] X. Xu, H. Xu, S. Mandal, R. Banerjee, S. Ghosh, and T. C. H. Liew, Interaction-induced double-sided skin effect in an exciton-polariton system, *Phys. Rev. B* **103**, 235306 (2021).
- [46] H. Xu, K. Dini, X. Xu, R. Banerjee, S. Mandal, and T. C. H. Liew, Nonreciprocal exciton-polariton ring lattices, *Phys. Rev. B* **104**, 195301 (2021).
- [47] D. Leykam, A. Andreanov, and S. Flach, Artificial flat band systems: From lattice models to experiments, *Adv. Phys.: X* **3**, 1473052 (2018).
- [48] B. Piętka, M. Molas, N. Bobrovska, M. Król, R. Mirek, K. Lekenta, P. Sępnicki, F. Morier-Genoud, J. Szczytko, B. Deveaud *et al.*, 2 s exciton-polariton revealed in an external magnetic field, *Phys. Rev. B* **96**, 081402(R) (2017).
- [49] B. Piętka, N. Bobrovska, D. Stephan, M. Teich, M. Król, S. Winnerl, A. Pashkin, R. Mirek, K. Lekenta, F. Morier-Genoud *et al.*, Doubly Dressed Bosons: Exciton Polaritons in a Strong Terahertz Field, *Phys. Rev. Lett.* **119**, 077403 (2017).
- [50] M. Mirhosseini, E. Kim, X. Zhang, A. Sipahigil, P. B. Dieterle, A. J. Keller, A. Asenjo-Garcia, D. E. Chang, and O. Painter, Cavity quantum electrodynamics with atom-like mirrors, *Nature (London)* **569**, 692 (2019).
- [51] J. A. Muniz, D. Barberena, R. J. Lewis-Swan, D. J. Young, J. R. Cline, A. M. Rey, and J. K. Thompson, Exploring dynamical phase transitions with cold atoms in an optical cavity, *Nature (London)* **580**, 602 (2020).
- [52] C. Ciuti, P. Schwendimann, and A. Quattropani, Theory of polariton parametric interactions in semiconductor microcavities, *Semicond. Sci. Technol.* **18**, S279 (2003).
- [53] W. Casteels, R. Rota, F. Storme, and C. Ciuti, Probing photon correlations in the dark sites of geometrically frustrated cavity lattices, *Phys. Rev. A* **93**, 043833 (2016).
- [54] B. Real, C. Cantillano, D. López-González, A. Szameit, M. Aono, M. Naruse, S.-J. Kim, K. Wang, and R. A. Vicencio, Flat-band light dynamics in stub photonic lattices, *Sci. Rep.* **7**, 15085 (2017).
- [55] M. Wouters and I. Carusotto, Probing the excitation spectrum of polariton condensates, *Phys. Rev. B* **79**, 125311 (2009).
- [56] S. Mandal, G.-G. Liu, and B. Zahng, Topology with memory in nonlinear driven-dissipative photonic lattices, *ACS Photonics* **10**, 147 (2023).
- [57] N. Bobrovska and M. Matuszewski, Adiabatic approximation and fluctuations in exciton-polariton condensates, *Phys. Rev. B* **92**, 035311 (2015).